RESEARCH ARTICLE OPEN ACCESS

The North Platte River Basin: Past, Present, and Future Patterns and Extremes in Streamflow

SallyRose Anderson*, Glenn Tootle**, Abdoul Oubeidillah***
** University of Tennessee, Knoxville*
*** University of Alabama*
**** University of Texas, Rio Grande Valley*
Corresponding Author: SallyRose Anderson

ABSTRACT
Evaluation of past, present, and future streamflow within the North Platte River Basin (NPRB) is presented. Reconstructed streamflow using tree rings provided a proxy for the long-term variability in the region. Observed (USGS) streamflow was used to analyze patterns and extremes in recent decades. Projected streamflow data from the Community Climate System Model (CCSM) was extracted to provide future insight of the hydroclimatic variability in the region. The streamflow reconstruction dated back to 1383 (617 years) and accounted for 69% of the overall variance. Drought analysis indicated numerous droughts occurred during the 1700s and only two droughts have occurred in the past century. Rescaling and mean bias correction methods were applied to adjust the CCSM streamflow datasets. A cyclical (10-year) correlation pattern was found between observed and modeled datasets. However, no significant trends were found when correlating the observed and modeled datasets with previous year major climate indices. Weibull exceedance probability plots were constructed to analyze the differences between past, present, and projected streamflow datasets. The average absolute difference between observed and modeled (CCSM) datasets for the overlapping period (1940–1999) was 7%, indicating CCSM modeled flow behaved similarly to observed flow. A1B projected streamflow implies the NPRB is currently in the wettest period in the next 100 years and the B1 scenario predicts the wettest period will occur within the next 20 years. Projected water-year streamflow from the A1B and A1FI datasets suggest the driest period will occur near the end of this century.
Keywords – Drought, Drought Forecasting, Streamflow, Tree Rings

Date of Submission: 28-02-2019 Date of acceptance: 25-03-2019

I. INTRODUCTION

The future challenges to provide water in the western U.S. are compounded by projections of continued population growth and forecasts of increased temperatures (climate change). The Intergovernmental Panel on Climatic Change (IPCC) noted the general pattern (trend) of drier conditions in the mid-latitudes and the consensus of these studies is increased temperatures will result in decreased streamflow. One of the most important impacts on society of future climatic changes will be changes in regional water availability. Such hydrologic changes will affect nearly every aspect of human well-being, from agricultural productivity and energy use to flood control, municipal and industrial water supply, and fish and wildlife management [1]. Improved understanding of the climate system could have substantial impact on the economic well-being of the nations of the world and numerous climate models have been developed to model future projections of atmospheric, biogeochemical, and hydrologic processes.

Few studies [2, 3] have been completed comparing reconstructed climate with projected climate. Furthermore, no study has been done comparing reconstructed streamflow with projected streamflow within a river basin. Increased value is added by comparing observed climate with projected and reconstructed climate because the length of the dataset is significantly lengthened. Evaluating the current and projected changes in climate provides important information for future mitigation and the management of water resources. However, the majority of recent studies are focused on climactic datasets over the past century based on instrumental records. Analyzing climactic patterns on a greater timescale (i.e., greater than 500 years based on a tree-ring reconstruction) is essential to understand current and future climate conditions. Forecasted changes in climate are often analyzed with respect to observational datasets because it is imperative to study and understand climate that has already occurred (observed climate) before making assumptions about climate that is projected to happen. However, most observational datasets have a relatively short period of record (~100 years). Reconstruction of past climates, based on multiple paleo indicators demonstrates that the historic record of roughly 100 years does not adequately capture the range of climatic variability observed during even the last 2000 years [4].

The first contribution developed a water-year streamflow reconstruction for the NPRB utilizing data developed from tree-ring records on a timescale (e.g., centennial) longer than the instrumental record. It was hypothesized that a successful streamflow reconstruction can be made in the NPRB based on the number of regional tree-ring chronologies available and the moisture sensitivity of western U.S. tree species. Additionally, valuable climate reconstructions have been published in surrounding regions [5, 6]. The second contribution evaluated past, present, and future temporal and spatial variability of climate systems and how they relate to extreme events (e.g., droughts in the NPRB). Past extremes were analyzed based on a streamflow reconstruction from tree-rings. Present extremes were analyzed based on instrumental streamflow data. Future extremes were analyzed based on projected climate model (i.e., CCSM) output data. It was hypothesized that the uncertainty with projected streamflow will be greater than the uncertainty associated with the reconstruction of streamflow, however, projected extremes in regional streamflow would have increased validation because it will be verified by a lengthened dataset. Furthermore, it was hypothesized that extreme events will be less intense in future years (i.e., 2010–2100) than projected because the lengthened dataset will show more hydroclimatic variability than what appears in the instrumental record. Finally, exceedance probability curves were constructed for each of the three periods (reconstructed, observed, and projected) to analyze the possible shifts in climate within the basin. While there are uncertainties in climate reconstructions and projected data from climate models, these datasets serve as the basis for policy and decision making and valuable information can still be extracted from them.

II. DATA

2.1 USGS Streamflow Data

Within the U.S., the United States Geological Survey (USGS) collects surface-water data that describe stream levels, streamflow (discharge), reservoir and lake levels, surface-water quality, and rainfall. Data is collected by automatic recorders and manual measurements. [7] identified a Hydro-Climatic Data Network (HCDN) of stream gages as being relatively free of significant human influences and, therefore, appropriate for climate studies. Streamflow measurements from one of these gages (USGS 06630000, Fig. 1) were incorporated in this study. The average water-year (October of previous year to September of following year) streamflow in the region was used in this study. This gage is important because it is the last streamflow gage before the North Platte flows through a series of five large reservoirs (with a combined capacity of 3.4 x 109 m3) that provide water supply and hydroelectric power for much of southern Wyoming [8]. Further downstream, the Platte River riparian corridor has been identified as critical habitat for several species of endangered birds and fish [9]. A principal focus of ecosystem restoration is controlled releases from upstream reservoirs [9, 10] which in turn depend strongly on seasonal reservoir inflows from headwater streams. Understanding the hydrology of the North Platte River headwaters is critically important for water resource planning in the Rocky Mountains and Great Plains regions [11].

2.2 Tree-Ring Data

Approximately 150 regional tree-ring chronologies were collected for the streamflow reconstruction. All ring width series were uniformly processed using the ARSTAN program [12] as follows. Measured series were standardized using conservative detrending methods (negative exponential/straight line fit or a cubic spline two thirds the length of the series) before using a robust weighted mean to combine all series into a single site chronology [13]. Low-order autocorrelation in the chronologies that may, in part, be attributed to biological factors [14] were removed, and the resulting residual chronologies were used.

2.3 CCSM Data

The projected streamflow dataset was extracted from the Community Land Model (CLM) within the Community Climate System Model (CCSM). Currently, the CCSM is a fully-coupled, global climate model that provides state-of-the-art computer simulations of the Earth’s past, present, and future climate studies. Model components within CLM include biogeophysics, hydrologic cycle, biogeochemistry, and dynamic vegetation. The model parameterizes interception, throughfall, canopy drip, snow accumulation and melt, water transfer between snow layers, infiltration, surface runoff, sub-surface drainage, and redistribution within the soil column to simulate changes in canopy water, snow water, soil water, and soil ice [15]. A river transport model (RTM) synchronously couples to the CLM for hydrologic applications (i.e., streamflow) as well as for improved land-ocean-sea-ice-atmosphere coupling in the CCSM. [15] provides a technical description of the CLM. Based on the resolution of the CCSM model, a single grid cell (Fig. 1) was used. Four CCSM streamflow datasets were collected. The first was the CCSM hindcast control run for the 20th century. This dataset was used to investigate the similarities and differences between observed and modeled streamflow. Projected CCSM streamflow datasets included the A1B, B1, and A1FI climate scenarios. A detailed description of these climate scenarios can be found in IPCC (2000).

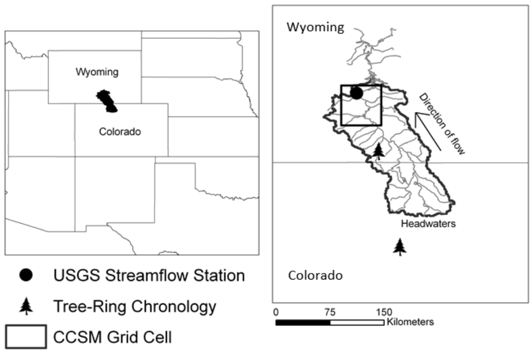

Figure 1: Location Map

III. METHODS

Water-year streamflow was obtained for three intervals. The first interval consisted of a newly developed streamflow reconstruction for the using tree-rings and provided streamflow data before the instrumental record. The instrumental streamflow record (1940–1999) comprised the second interval. The last interval consisted of projected streamflow data from CCSM (2001–2099).

3.1 Reconstruction Methods

The period of 1940–1999 (n = 60) was used for model calibration and verification. Significant (95%) and stable tree chronologies were considered as initial predictors in model calibration. Stability analysis consisted of performing a 10-year moving correlation window, similar to [16], between streamflow and tree-ring widths. Chronologies containing insignificant 10-year r-values were removed from analysis. Regression approaches are the most common statistical method in climate reconstructions. In the simplest case, a linear regression equation is used to reconstruct past values of a single climatic variable from ring-width indices of a single tree-ring chronology, or from a mean of two or more chronologies which have been merged to form a single chronology [17]. Following the procedure of [5], the F level for a predictor was allowed to have a maximum p value of 0.05 for entry and 0.10 for retention in the stepwise regression model. Verification statistics calculated to check for model validation included R^2, R^2-predicted, Variance Inflation Factor (VIF), and the Durbin-Watson statistic. R^2 measures the proportion of variation in the response that is accounted for by the predictor variables; a higher R^2 indicates a better fit of the model to the data. R^2-predicted is calculated from the Predicted REsidual Sums of Squares (PRESS) statistic. PRESS is based upon a leave-one-out cross-validation in which a single year or observation is removed when fitting the model. As a result, the prediction errors are independent of the predicted value at the removed observation [18]. VIF indicates the extent to which multicollinearity is present in a regression analysis. A VIF value close to 1.0 indicates low correlation between predictors, and is the ideal value for a reconstruction model. The Durbin-Watson statistic was used to analyze the autocorrelation structure of model residuals. It was imperative that the predictor chronologies and reconstruction residuals contained similar autocorrelation structures for model validation. The length of the streamflow reconstruction was directly related to the age of the chronologies retained by the stepwise regression model.

3.2 Statistical Analysis

Calculated statistical parameters for each streamflow time series included mean, median, minimum, and maximum. Annual, 5-year, and decadal extreme periods were also determined. The significance and reliability of past and projected extreme events depended on the uncertainty associated with each calibrated model. The presented methods determined the direct effect climate change is projected to have on water resources within the NPRB based on an extended period of record (>500 years).

3.3 Weibull Exceedance Probability

The most efficient formula for computing plotting positions for unspecified distributions and the one now commonly used for most sample data, is the Weibull equation [19]:

$$P = m/(n+1) \ldots\ldots. (1)$$

where m is the rank of descending values and n is the number of values. P is an estimate of the probability of values being equal to or more than the ranked value. Weibull exceedance probability plots provide water managers good estimates of average flows as well as extreme flows. Weibull plots were constructed to analyze possible shifts in flow regimes between past, present, and projected flow within the NPRB.

IV. RESULTS

4.1 Reconstruction Results and Drought Analysis

Two water-year streamflow reconstructions were found to be feasible in the region (Table 1).

Reconstruction possibilities were as follows: 1487 (three chronology predictors retained by stepwise regression); 1383 (two chronology predictors). We determined that reconstructing streamflow back to 1383 (617 years) in the region would provide the most value based on the length of the reconstruction and the predictability (R^2-predicted) of the model. The calibrated model (Fig. 2) explained 69% of the overall variance in water-year streamflow records from 1940–1999. The Variance Inflation Factor (VIF) and Durbin-Watson statistic concluded there were no issues with multicollinearity and autocorrelation, respectively. The two chronologies (Fig. 1) retained after performing stepwise regression were Encampment, a Douglas-fir species (Pseudotsuga menziesii M.) and Pumphouse (Pinus edulis E.).

Table 1: Streamflow reconstruction verification and validation statistics.

	3-Predictor Model	2-Predictor Model
Date of Reconstruction	1487	1383
R^2	0.71	0.69
R^2 - predicted	0.68	0.66
VIF	1.63	1.08
Durbin-Watson	1.85	1.86

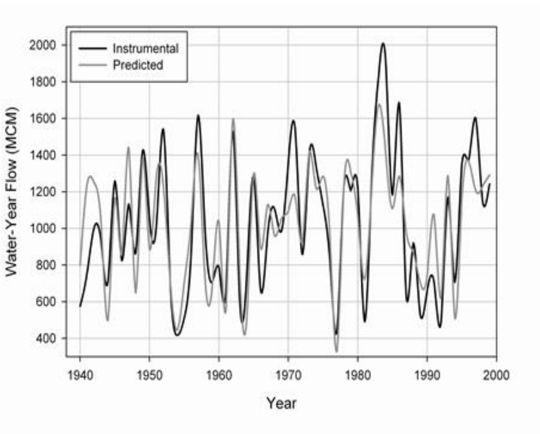

Figure 2: Calibrated Reconstruction Model explaining 69% of the variance in streamflow records.

Reconstructed water-year streamflow in the NPRB, smoothed with five and 25-year filters is shown in Fig. 3. A noticeable oscillation (e.g., around 30 years) was found to occur based on the reconstruction. This oscillation began at the beginning of the reconstruction (1383) and continued to 1700. The oscillation is less evident for the next 200 years but appears to begin again around 1900 and continue to the end of the reconstruction. Possible explanations for this oscillation are discussed in subsequent sections. Extreme (drought) events in past centuries based on the reconstruction were determined applying a simple technique. A drought was defined as a period of at least 3 years in which the water-year streamflow was below the overall average. Two main findings were discovered: droughts occurred most frequently in the 1700s while only two droughts occurred in the past century based on the reconstruction (Fig. 4).

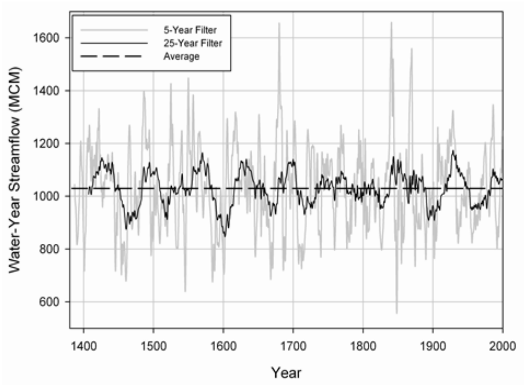

Figure 3: Complete streamflow reconstruction smoothed with five- and 25-year filters.

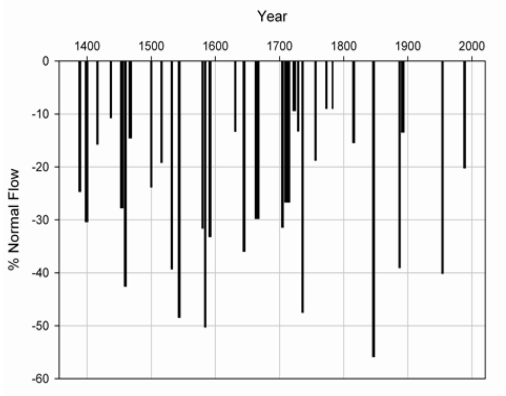

Figure 4: Periods of drought found in the past 600 years in the NPRB, based on the streamflow reconstruction, where the length of each bar represents the severity of the drought while the width represents the length of the drought.

4.2 CCSM Rescaling and Bias Correction

Differences in streamflow magnitude were found between observed (USGS) and modeled (CCSM) datasets. Two methods were applied to adjust (i.e., correct) modeled streamflow data from CCSM. First, a rescaling method was applied [20, 21]. CCSM streamflow values before the instrumental record (1871–1939) were rescaled to have the same variance as reconstructed flow (i.e., paleo-conditioned). CCSM streamflow values during the instrumental record (1940–2009) were rescaled to have the same variance as observed flow. The mean of the CCSM series was subtracted from each value. Each centered observation was then multiplied by a scaling factor, k, defined as:

k = sx / sp………(2)

where sx is the standard deviation of the observed or reconstructed values (depending on the period) and sp is the standard deviation of the modeled values. Finally, the mean was added back to each modeled value. The rescaling method applied results in more realistic modeled streamflow without affecting the overall correlation between datasets. To correct the bias (i.e., magnitude) within the CCSM streamflow dataset, the average difference between the observed or reconstructed dataset (depending on the period) and modeled dataset was added to the modeled dataset. Projected CCSM flows were rescaled based on the mean and standard deviation of observed flow only.

The overall correlation between observed (USGS) and modeled (CCSM) streamflow from 1940–1999 was not significant. This result was not unexpected based on the uncertainties and resolution of current climate models. However, when analyzed further, an important discovery was found. When performing a 10-year moving correlation window on the datasets, an oscillation appeared (Fig. 5). There were periods in which the datasets behaved opposite and similarly to each other. This was first discovered between the instrumental and modeled datasets (1940–1999). Using the reconstruction, this oscillation was found to continue back to the beginning of the modeled dataset (1871). Confirming these results is the period of 2000–2010 in which the observed and projected (A1B) datasets maintain the oscillation. A possible explanation for this oscillation as well as the oscillation found in the reconstruction was hypothesized to be the influence of climate indices (AMO/PDO/ENSO) on regional streamflow. To investigate this oscillation in more depth, observed and modeled flows were correlated with major climate indices. Previous year climate indices were correlated with following year streamflow to determine the possibility of sea surface influence on observed and modeled flow in the region. However, virtually all correlation values were found to be insignificant between streamflow and the major sea surface oscillations. The only significant (95%) outcome occurred between previous year AMO and following year reconstructed streamflow values. It is unknown to the authors the cause of this 10-year oscillation between observed and modeled flows, however this finding should assist in the improvement of modeled CCSM streamflow.

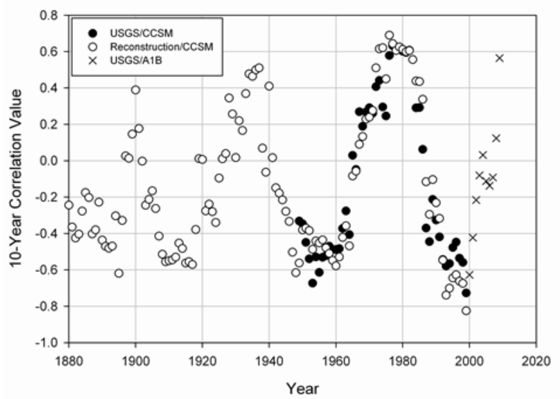

Figure 5: 10-year correlation plot showing an oscillation found between observed and modeled water-year flows from 1880 - 2009.

4.3 Weibull Exceedance Probability

Weibull exceedance probability plots were created during the overlapping period (1940–1999) for observed and reconstructed flows (Fig. 6) and observed and modeled (CCSM) flows (Fig. 7). The reconstruction model tended to overestimate low flows and underestimate high flows. The average absolute difference between observed and reconstructed flows was 7%. While there was no significance between observed and modeled flow based on correlation, the average absolute difference from the Weibull distribution was also 7% between the datasets, indicating that the modeled data follows a similar flow regime to observed data (Fig. 7). This similarity also suggests that projected modeled flows from CCSM can be analyzed with comparable accuracy and uncertainty. Furthermore, CCSM tended to overestimate extreme flows while underestimating average flows. A Weibull exceedance probability was created comparing observed flows with projected flows (Fig. 8). Projected flows included three climate scenarios: A1B, B1, and A1FI. Results indicate relatively minor deviations between instrumental and projected flow patterns. Most differences occurred below the exceedance probability of 60%. This indicates low flows are projected to remain close to the same while higher flows are expected to change slightly (Fig. 8).

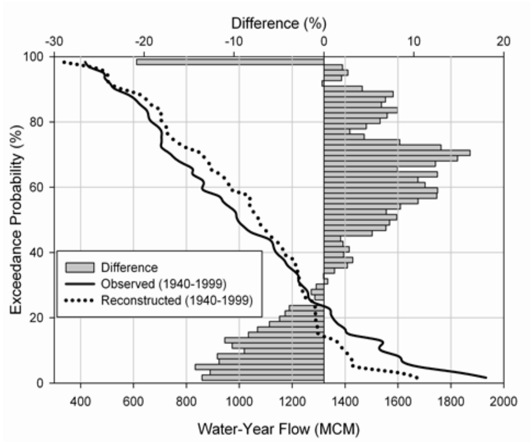

Figure 6: Weibull exceedance probability plot for observed and reconstructed water-year flow during the calibrated period (1940-1999) where reconstructed flow overestimates low flows and underestimates high flows.

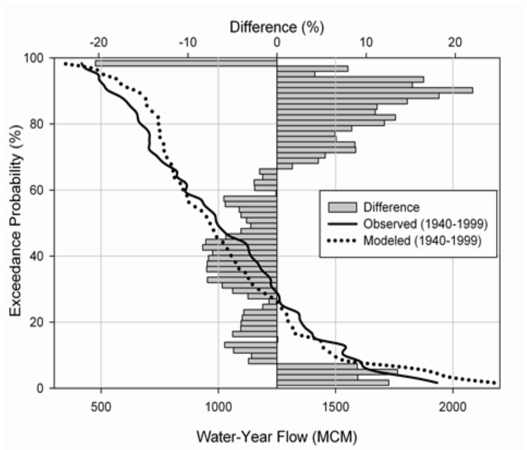

Figure 7: Weibull exceedance probability for observed and modeled water-year flow during the calibrated period (1940-1999) where modeled flow overestimated extreme flows and underestimates average flows.

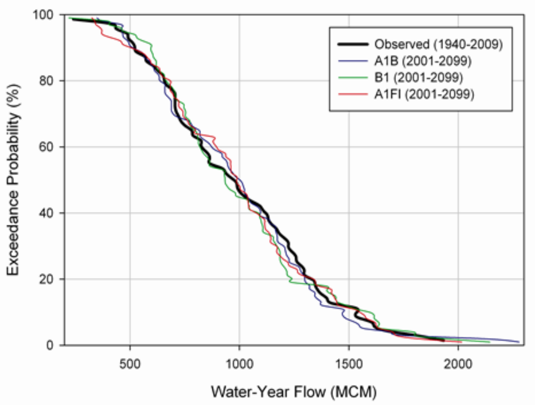

Figure 8: Weibull exceedance probability plot for observed and projected water-year flow based on three difference climate scenarios.

V. EVALUATION OF PAST, PRESENT, AND FUTURE CLIMATE IN THE NORTH PLATTE RIVER BASIN

Streamflow extremes and patterns within the NPRB based on reconstructed, instrumental, and projected datasets (Tables 2 and 3) was evaluated from 1383–2099. The streamflow reconstruction contains the highest annual flow value of all datasets, and it occurred in 1843. This year was the last of the wettest 10-year period (1835–1844). However, the driest 5-year period during the reconstructed record started the following year (1844–1848). The instrumental dataset indicates that 2002 was the driest year on record and 1984 was the wettest year on record. Furthermore, the driest consecutive years on record within the NPRB occurred in the past 12 years (1998–2007) and the wettest time was from 1978–1987.

Table 2: Reconstructed and instrumental water-tear streamflow statistics and extreme periods.

Units = MCM	Reconstruction	Instrumental
Period	1383-1939	1940-2009
Mean	1030.2	995.5
Median	1042.0	972.8
Min (Year)	6.4 (1842)	241.5 (2002)
Max (Year)	2560.8(1843)	1933.0 (1984)
Driest Periods		
5-year (Years)	583.3 (1844-1848)	553.3 (2000-2004)
10-year (Years)	715.8 (1452-1461)	786.8 (1998-2007)
Wettest Periods		
5-year (Years)	1655.9 (1676-1680)	1576.7 (1982-1986)
10-year (Years)	1401.9 (1835-1844)	1265.5 (1978-1987)

Table 3: Projected water-year streamflow statistics and extreme periods.

Units = MCM	A1B	B1	A1FI
Period	2001-2099	2001-2099	2001-2099
Mean	995.5	995.5	995.5
Median	1001.7	934.4	987.9
Min (Year)	349.4(2071)	220.7 (2031)	325.4(2093)
Max (Year)	2277.5(2055)	2144.1 (2029)	2015.5(2070)
Driest Periods			
5-year (Years)	664.9(2086-2090)	732.0 (2051-2055)	650.4(2091-2095)
10-year (Years)	772.1(2086-2095)	789.6 (2045-2054)	686.3(2085-2094)
Wettest Periods			
5-year (Years)	1322.0(2007-2011)	1361.2 (2011-2015)	1488.0(2019-2023)
10-year (Years)	1306.5(2007-2016)	1286.1 (2021-2030)	1337.3(2064-2073)

The authors acknowledge projected climate contains more uncertainties than reconstructed climate, however, it should be noted that interesting similarities and differences in streamflow within the NRPB were discovered between the three climate scenarios. Based on the rescaling methods applied in this study, differences in magnitude between observed and projected streamflow was not considered. Instead, possible periods in which extreme streamflow is projected to occur was examined (Fig. 9). The A1B and A1FI datasets agree on when the driest phase will likely occur in the next 100 years. Both scenarios suggest the driest time will occur near the end of the century (2085–2095). The A1B scenario projects that the NRPB is currently in the wettest period of the century (2007–2016) and the B1 scenario suggests the wettest period is likely to occur within the next 20 years (2011–2030). Contrary to the A1B and A1FI scenarios, the B1 scenario projects the driest period to occur from 2045–2055. The wettest 5-year period from the A1FI scenario is also likely to occur in the next 20 years (2019–2023) but the wettest 10-year period is projected to occur from 2064–2073.

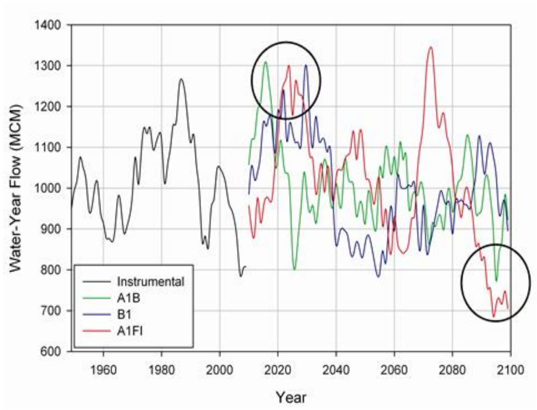

Figure 9: Projected water-year streamflow smoothed with a 10-year filter, showing that the wettest period is most likely to occur within the next 20 years while the driest period is projected to happen near the end of the century.

VI. CONCLUSIONS

A thorough study has been completed evaluating the past, present, and future climate within the NPRB. The first accurate climate reconstruction was developed for the region and explained 69% of the variance in streamflow records. Drought analysis was performed on the reconstructed record and discovered numerous drought periods, most notably during the 1700s. Based on the streamflow reconstruction, only two droughts have occurred in the past century with respect to the lengthened dataset. Weibull exceedance probability plots were created to analyze possible shifts in the flow regime of the basin. Modeled streamflow data from CCSM was rescaled and used to recognize when extreme events are most likely to occur in the next century. It was discovered that the NPRB is likely to experience the wettest period of this century in the next 20 years. Two of the three climate scenarios suggest the driest time is projected to occur in the last 20 year of this century. As the resolution of climate models become finer and water cycle algorithms become more accurate, future streamflow predictions of streamflow within the NPRB can compared to the findings presented here. Future work may apply a downscaling method into a physical model to obtain more accurate projected streamflow in the region. Lastly, the methods and concepts presented in this research can be applied to any region in which successful climate reconstructions can be attained to examine past, present, and projected climate variables.

ACKNOWLEDGEMENTS

The authors would like to acknowledge the assistance provided by Dr. Cody Moser, former PhD student at the University of Tennessee, Knoxville.

REFERENCES

[1]. Chong-yu, X., 1999. From GCMs to river flow: a review of downscaling methods and hydrologic modelling approaches. Progress in Physical Geography, 23, 229, doi: 10.1177/030913339902300204.

[2]. Girardin, M.P. and Mudelsee, M., 2008. Past and future changes in Canadian boreal wildfire activity. Ecological Applications, 18(2), 391–406.

[3]. Tchebakova, N.M., Blyakharchuk, T.A., and Parfenova, E.I., 2009. Reconstruction and prediction of climate and vegetation change in the Holocene in the Altai-Sayan mountains, Central Asia. Environmental Research Letters, 4(4), 045025, doi:10.1088/1748-9326/4/4/045025.

[4]. Lemmen, D.S., Vance R.E., Wolfe, S.A., and Last, W.M., 1997. Impacts of future climate change on the southern Canadian prairies: A paleoenvironmental perspective. Geoscience Canada, 24(3), 121–133.

[5]. Woodhouse, C.A., S.T. Gray, and D.M. Meko, 2006. Updated Streamflow Reconstructions for the Upper Colorado River Basin. Water Resources Research 42(5):WO5415, doi: 10.1029/2005WR004455.

[6]. Meko, D.M., C.A. Woodhouse, C.A. Baisan, T. Knight, J.J. Lukas, M.K. Hughes, and M.W. Salzer, 2007. Medieval Drought in the Upper Colorado River Basin. Geophysical Research Letters 34(10):L10705, doi:10.1029/2007GL029988.

[7]. Slack, J.R., and Landwehr, J.M., 1992. Hydro-Climatic Data Network: A U.S. Geological Survey streamflow data set for the United States for the study of climate variations, 1874–1988. USGS Open-File Report 92–129, 193.

[8]. Ostresh, L.M., Jr., Marston, R.A., Hudson, W.M., 1990. Wyoming Water Atlas. Wyoming Water Development Commission, Laramie, WY, pp. 124.

[9]. National Research Council (NRC), 2004. Endangered and Threatened Species of the Platte River. National Academics Press, Washington, DC, pp. 336.

[10]. Graf, W.L., 2001. Damage control: restoring the physical integrity of America's rivers. Annals of the Association of American Geographers, 91, 1–27.

[11]. Daniels, J.M., 2007. Flood hydrology of the North Platte headwaters in relation to precipitation variability. Journal of Hydrology, 344(1–2), 70–81, doi:10.1016/j.jhydrol.2007.06.020.

[12]. Cook, E.R, 1985. A Time Series Approach to Tree-Ring Standardization, Ph.D. dissertation. University of Arizona., Tucson.

[13]. Cook, E.R., K. Briffa, S. Shiyatov, and V. Mazepa, 1990. Tree-Ring Standardization and Growth-Trend Estimation. In: Methods of Dendrochronology: Applications in the Environmental Sciences, E.R. Cook and L.A. Kairukstis. (Editors). Springer, New York.

[14]. Fritts, H.C., 1976. Tree Rings and Climate. Academic Press, London, United Kingdom.

[15]. Oleson, K.W., Dai, Y., Bonan, G., Bosilovich, M., Dickinson, R., Dirmeyer, P., Hoffman, F., Houser, P., Levis, S., Niu, G.Y., Thornton, P., Vertenstein, M., Yang, Z.L., Zeng, X., 2004. Technical Description of the Community Land Model (CLM). NCAR Technical Note (NCAR/TN-461+STR).

[16]. Biondi, F., and K. Waikul. 2004. DENDROCLIM2002: A C++ program for statistical calibration of climate signals in tree-ring chronologies. Computers and Geosciences 30(3): 303–311.

[17]. Blasing, T.J., D.N. Duvick, and D.C. West, 1981. Dendroclimatic Calibration and Verification Using Regionally Averaged and Single Station Precipitation Data. Tree-Ring Bulletin 41:37–43.

[18]. Garen, D.C., 1992, Improved techniques in regression-based streamflow volume forecasting. Journal of Water Resources Planning and Management, 118(6), 654–670.

[19]. Viessman, W. and Lewis, G.L, 2003. Introduction to Hydrology. 5th ed. Pearson Education, Inc., Upper Saddle River, New Jersey, USA.

[20]. Graumlich, L.J., 1987. Precipitation Variation in the Pacific Northwest (1675–1975) as Reconstructed from Tree Rings. Annals of the Association of American Geographers 77(1):19–29.

[21]. Grissino-Mayer, H.D., 1989. Climatic Response in Tree Rings of Loblolly Pine from North Georgia. Physical Geography, 10(1):32–43.

SallyRose Anderson" The North Platte River Basin: Past, Present, and Future Patterns and Extremes in Streamflow" International Journal of Engineering Research and Applications (IJERA), Vol. 09, No.03, 2019, pp. 01-08